

## Supplementary Materials for

### **INTS11 regulates hematopoiesis by promoting PRC2 function**

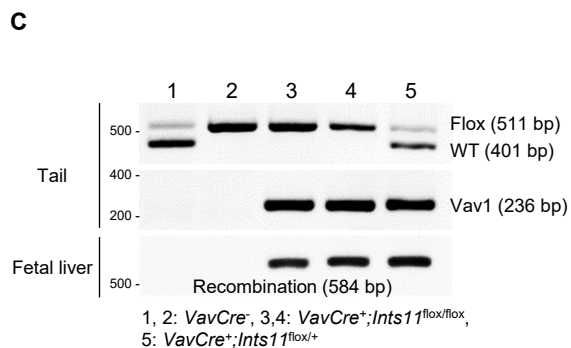
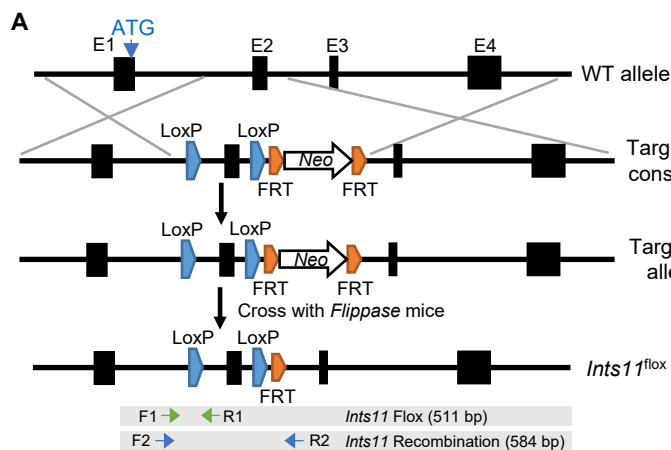
Peng Zhang\*, Pinpin Sui, Shi Chen, Ying Guo, Ying Li, Guo Ge, Ganqian Zhu, Hui Yang,  
Cody M. Rogers, Patrick Sung, Stephen D. Nimer, Mingjiang Xu, Feng-Chun Yang\*

\*Corresponding author. Email: yangf1@uthscsa.edu (F.-C.Y.); zhangp1@uthscsa.edu (P.Z.)

Published 1 September 2021, *Sci. Adv.* 7, eabh1684 (2021)  
DOI: 10.1126/sciadv.abh1684

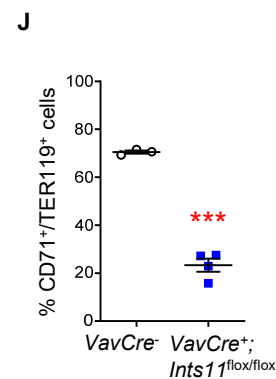
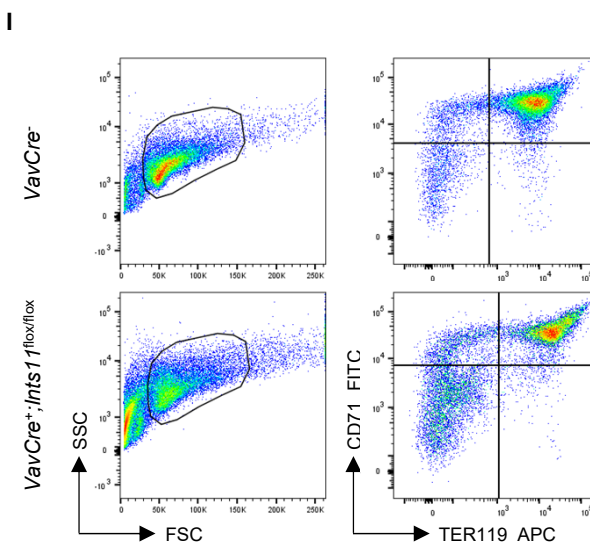
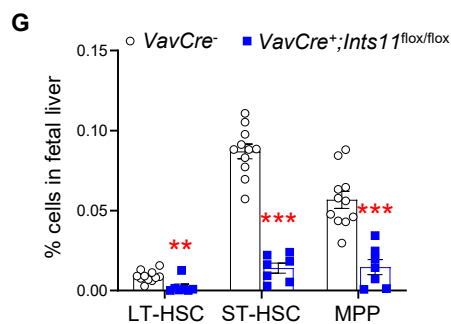
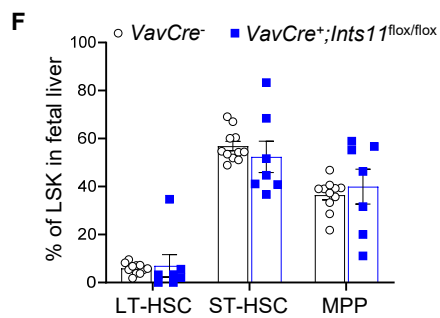
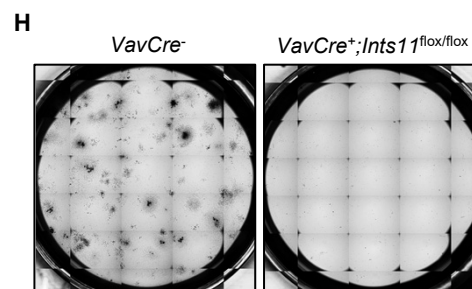
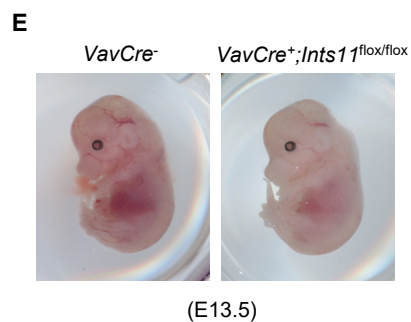
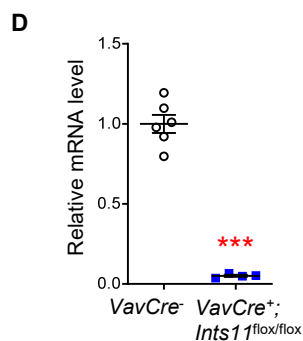
#### **This PDF file includes:**

Figs. S1 to S8  
Tables S1 and S2

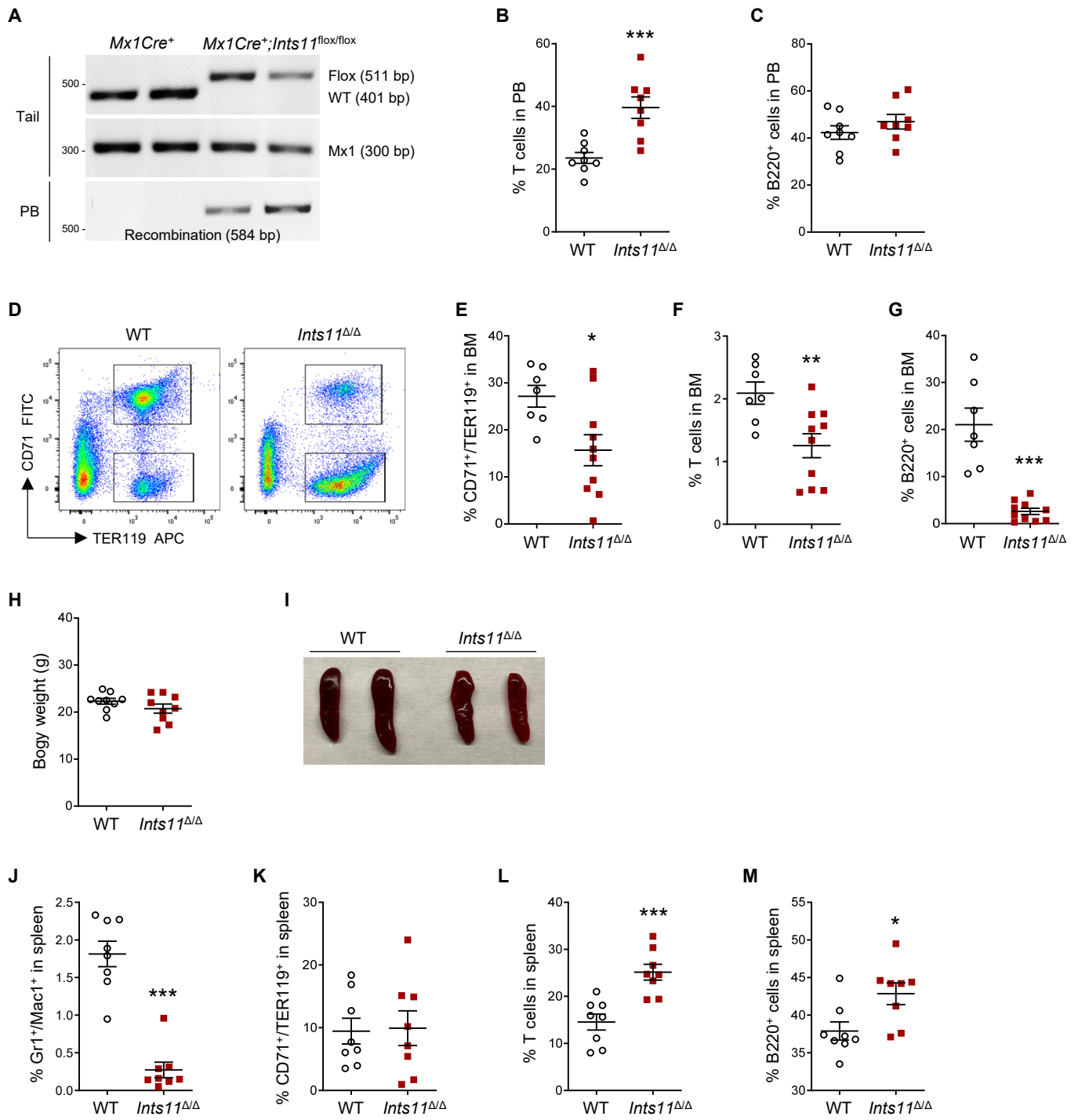


**B**

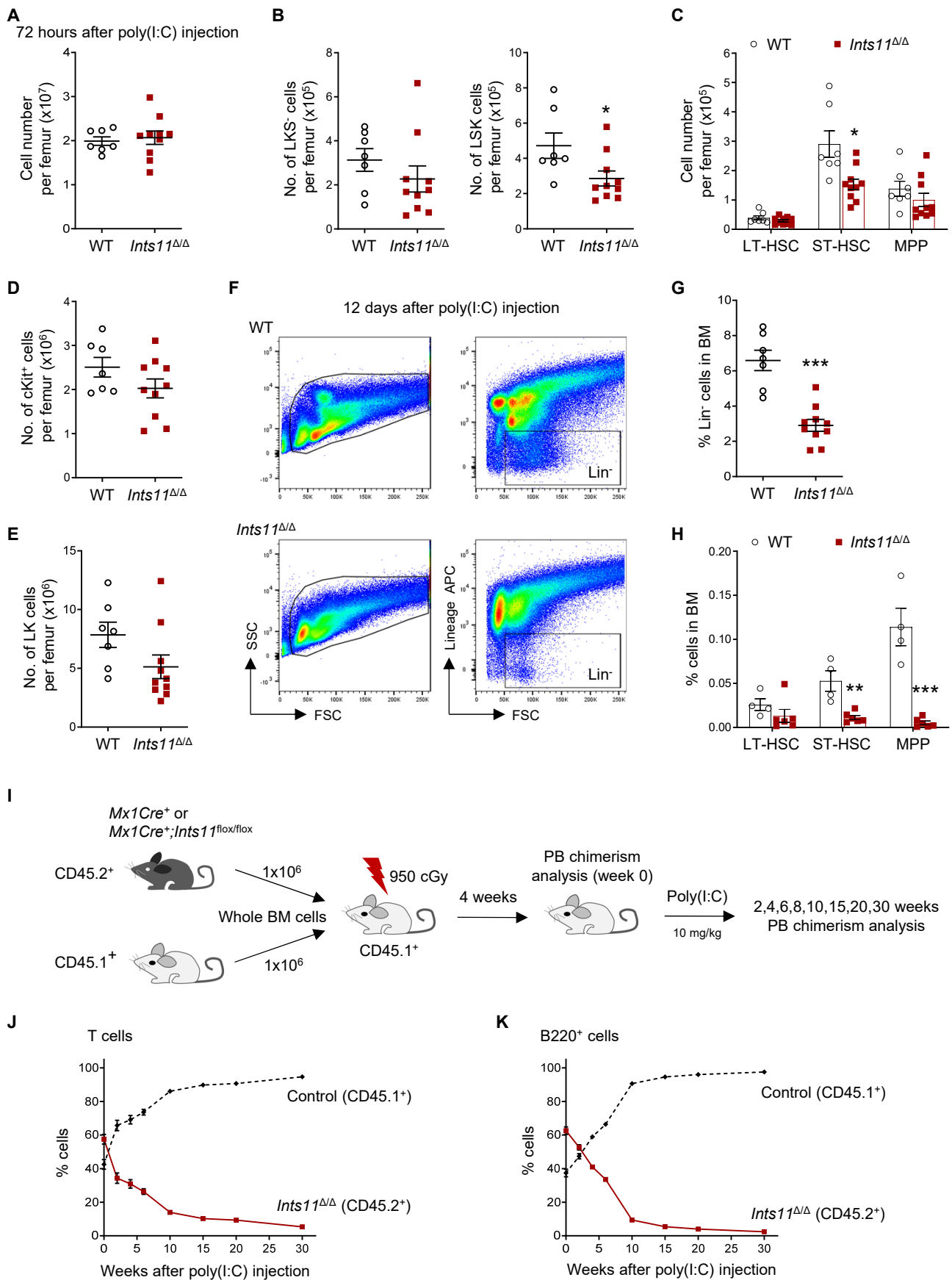
		<i>VavCre</i> <sup>-</sup>	<i>VavCre</i> <sup>+</sup> ; <i>Ints11</i> <sup>lox/+</sup>	<i>VavCre</i> <sup>+</sup> ; <i>Ints11</i> <sup>lox/lox</sup>
	Expected	50%	25%	25%
E13.5	Observed (n = 44)	50.0% (n = 22)	22.7% (n = 10)	27.3% (n = 12)
E14.5	Observed (n = 40)	52.5% (n = 21)	25.0% (n = 10)	22.5% (n = 9)
E15.5	Observed (n = 34)	44.1% (n = 15)	32.4% (n = 11)	23.5% (n = 8)
E16.5	Observed (n = 35)	57.1% (n = 20)	14.3% (n = 5)	28.6% (n = 10)
E17.5	Observed (n = 37)	59.4% (n = 22)	18.9% (n = 7)	21.6% (n = 8)
E18.5	Observed (n = 22)	50.0% (n = 11)	40.9% (n = 9)	9.09% (n = 2)



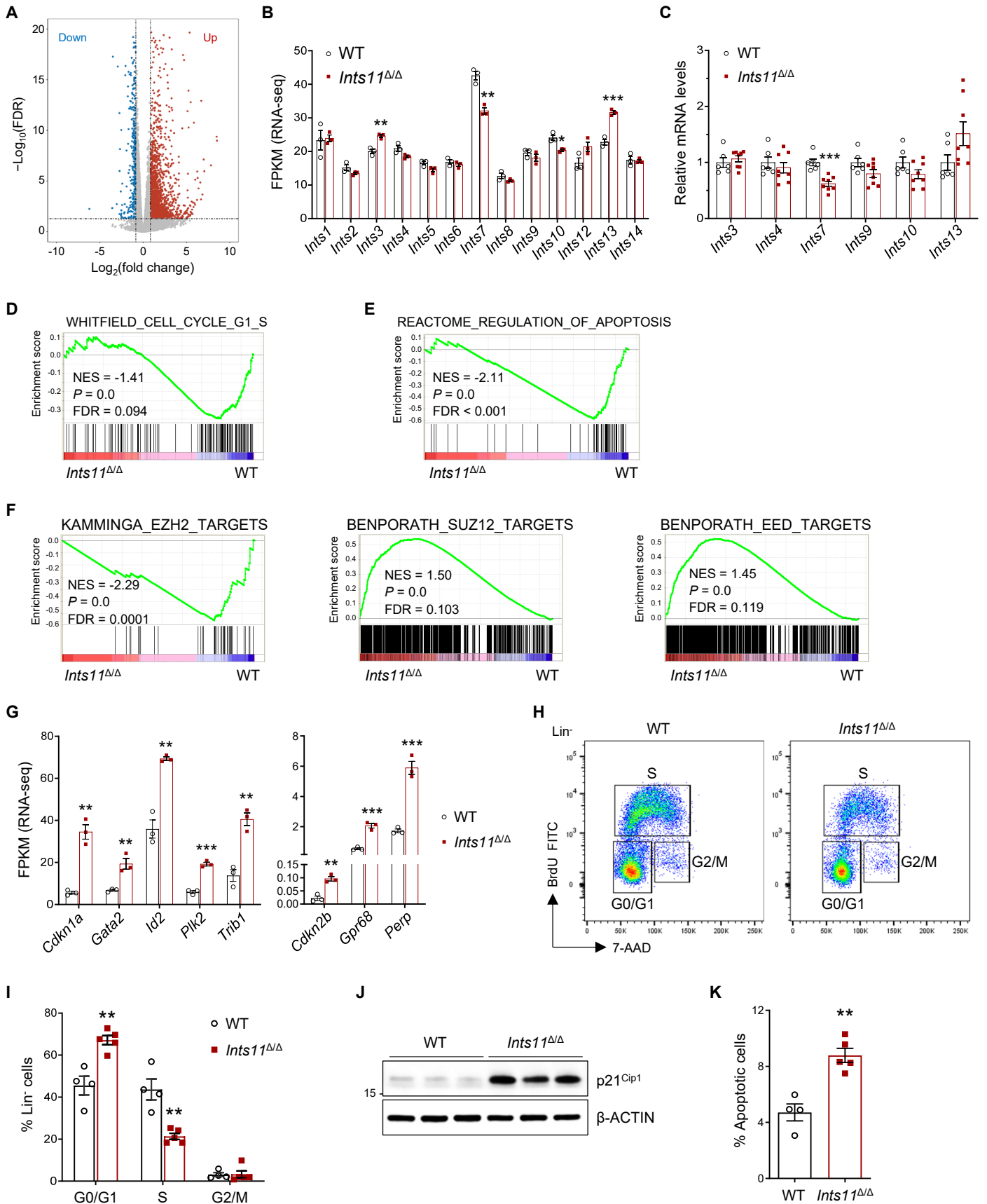
**Fig. S1. INTS11 is required for fetal hematopoiesis.** (A) Schematic of the targeted mouse *Ints11* allele. Targeting vector contained exon 2 flanked by LoxP sites (blue) and a neomycin resistance gene flanked by FRT (orange). The locations of primers are shown. (B) Genotype analysis of embryos after mating of *Vav1Cre<sup>+</sup>;Ints11<sup>flox/+</sup>* (female) x *Vav1Cre<sup>-</sup>;Ints11<sup>flox/flox</sup>* (male) mice. (C) Genotyping of *Vav1Cre<sup>+</sup>;Ints11<sup>flox/flox</sup>* embryos and controls. (D) mRNA levels of *Ints11* in fetal liver CD45<sup>+</sup> cells from *Vav1Cre<sup>-</sup>* ( $n = 6$ ) and *Vav1Cre<sup>+</sup>;Ints11<sup>flox/flox</sup>* ( $n = 4$ ) embryos at E13.5. (E) Representative images of E13.5 embryos from *Vav1Cre<sup>+</sup>;Ints11<sup>flox/flox</sup>* and control littermates. Photo Credit: Peng Zhang, University of Texas Health Science Center at San Antonio. (F and G) Quantification of the percentages of LT-HSC, ST-HSC, and MPP cell populations from control ( $n = 11$ ) and *Vav1Cre<sup>+</sup>;Ints11<sup>flox/flox</sup>* ( $n = 7$ ) fetal livers at E13.5. LT-HSC, Lin<sup>-</sup>Sca1<sup>+</sup>cKit<sup>+</sup>CD34<sup>-</sup>CD135<sup>-</sup>; ST-HSC, Lin<sup>-</sup>Sca1<sup>+</sup>cKit<sup>+</sup>CD34<sup>+</sup>CD135<sup>-</sup>; MPP, Lin<sup>-</sup>Sca1<sup>+</sup>cKit<sup>+</sup>CD34<sup>+</sup>CD135<sup>+</sup>. (H) Representative images of colony formation for fetal liver cells from *Vav1Cre<sup>+</sup>;Ints11<sup>flox/flox</sup>* and controls are shown. The images were taken on the 7<sup>th</sup> day of the assay. (I) Flow cytometric analysis of erythroid cells from control and *Vav1Cre<sup>+</sup>;Ints11<sup>flox/flox</sup>* fetal livers at E13.5. (J) Quantification of the percentages of CD71<sup>+</sup>/TER119<sup>+</sup> cells from control ( $n = 3$ ) and *Vav1Cre<sup>+</sup>;Ints11<sup>flox/flox</sup>* ( $n = 4$ ) fetal livers at E13.5. Data are shown as the mean  $\pm$  SEM. Unpaired Student's *t*-test; \*\* $P < 0.01$ , \*\*\* $P < 0.001$ .



**Fig. S2. INTS11 deletion leads to hematopoietic failure.** (A) Genotyping of *Mx1Cre<sup>+</sup>;Ints11<sup>flox/flox</sup>* (*Ints11<sup>Δ/Δ</sup>*) and *Mx1Cre<sup>+</sup>* (WT) control mice. (B and C) Frequencies of T (CD4<sup>+</sup>, CD8<sup>+</sup>, and CD4<sup>+</sup>/CD8<sup>+</sup>, B) and B cells (B220<sup>+</sup>, C) in PB from WT and *Ints11<sup>Δ/Δ</sup>* mice (*n* = 8 per genotype) 12 days after poly(I:C) injection. (D) Flow cytometric analysis of erythroid cells in BM from WT and *Ints11<sup>Δ/Δ</sup>* mice 12 days after poly(I:C) injection. (E-G) Frequencies of erythroid (CD71<sup>+</sup>/TER119<sup>+</sup>, E), T (CD4<sup>+</sup>, CD8<sup>+</sup>, and CD4<sup>+</sup>/CD8<sup>+</sup>, F) and B cells (B220<sup>+</sup>, G) in BM from WT (*n* = 7) and *Ints11<sup>Δ/Δ</sup>* mice (*n* = 10) are shown. (H) Body weight of WT and *Ints11<sup>Δ/Δ</sup>* mice (*n* = 9 per genotype) 12 days after first poly(I:C) injection. (I) The gross appearance of spleen from WT and *Ints11<sup>Δ/Δ</sup>* mice. Photo Credit: Peng Zhang, University of Texas Health Science Center at San Antonio. (J-M) Frequencies of myeloid cells (Gr1<sup>+</sup>/Mac1<sup>+</sup>, J), erythroid cells (CD71<sup>+</sup>/TER119<sup>+</sup>, K), T cells (CD4<sup>+</sup>, CD8<sup>+</sup>, and CD4<sup>+</sup>/CD8<sup>+</sup>, L), and B cells (B220<sup>+</sup>, M) in the spleens from WT and *Ints11<sup>Δ/Δ</sup>* mice (*n* = 8 per genotype) 12 days after poly(I:C) injection. Data are shown as the mean ± SEM. Unpaired Student's *t*-test; \**P* < 0.05, \*\**P* < 0.01, \*\*\**P* < 0.001.



**Fig. S3. Loss of *Ints11* results in HSPC defects and impairs hematopoietic reconstitution.** (A) BM cellularity of WT ( $n = 7$ ) and *Ints11*<sup>Δ/Δ</sup> mice ( $n = 10$ ) 72 hours after first poly(I:C) injection. (B-E) Absolute number of HSPC populations from WT ( $n = 7$ ) and *Ints11*<sup>Δ/Δ</sup> mice ( $n = 10$ ) 72 hours after poly(I:C) injection are shown. (F) Flow cytometric analysis of lineage negative (Lin<sup>-</sup>) cells in BM from WT and *Ints11*<sup>Δ/Δ</sup> mice 12 days after first poly(I:C) injection. (G) Quantification of the percentage of Lin<sup>-</sup> cells in total BM cells from WT ( $n = 7$ ) and *Ints11*<sup>Δ/Δ</sup> mice ( $n = 10$ ) 12 days after poly(I:C) injection. (H) The percentages of LT-HSC, ST-HSC, and MPP in total BM cells from WT ( $n = 4$ ) and *Ints11*<sup>Δ/Δ</sup> mice ( $n = 6$ ) 12 days after poly(I:C) injection are shown. Data are shown as the mean ± SEM. Unpaired Student's *t*-test; \* $P < 0.05$ , \*\* $P < 0.01$ , \*\*\* $P < 0.001$ . (I) Schematic for competitive repopulation assay. CD45.2<sup>+</sup> BM cells from *Mx1Cre*<sup>+</sup> or *Mx1Cre*<sup>+</sup>;*Ints11*<sup>flox/flox</sup> mice were mixed with equal numbers of CD45.1<sup>+</sup> competitor cells and transplanted into lethally irradiated CD45.1<sup>+</sup> recipient mice. *Ints11* deletion was induced upon confirmation of comparable engraftment rates. (J and K) The percentages of *Ints11*<sup>Δ/Δ</sup>-derived (CD45.2<sup>+</sup>) versus CD45.1<sup>+</sup> cells in the populations of T cell (J) and B cell (K) from PB of recipient animals at indicated time points ( $n = 4$ ).

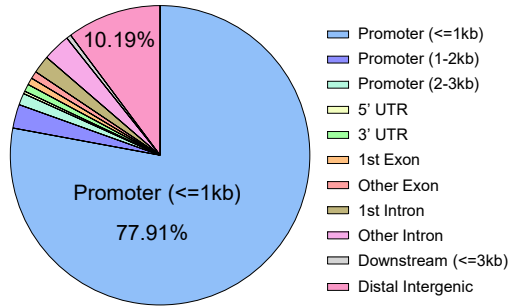
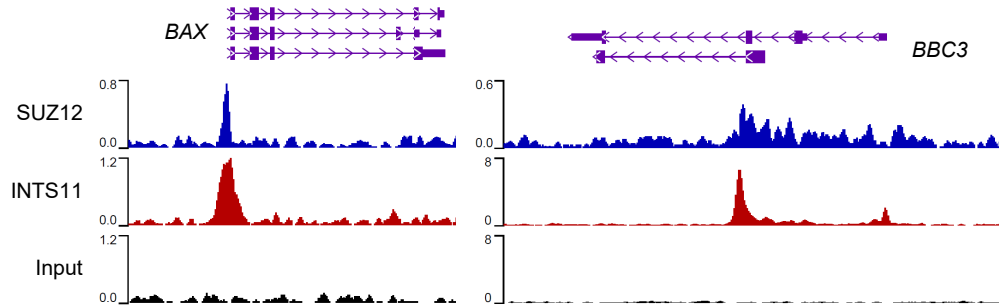
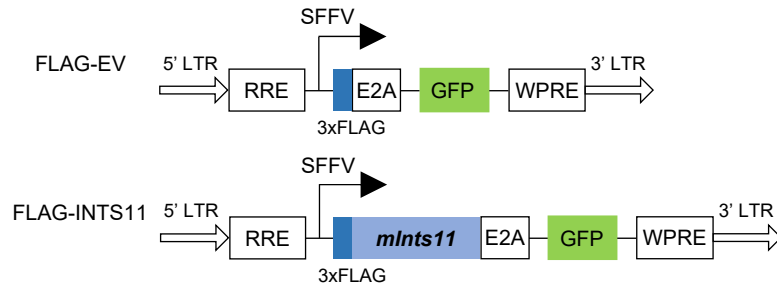
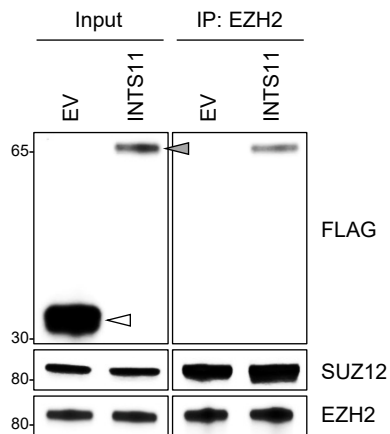
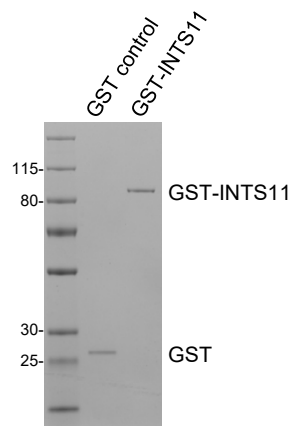
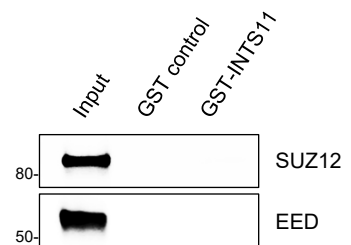




**Fig. S4. Loss of *Ints11* derepresses PRC2 target genes in HSPCs.** (A) Volcano plot showing the significantly dysregulated genes in *Ints11*<sup>Δ/Δ</sup> Lin<sup>-</sup>cKit<sup>+</sup> (LK) cells compared with WT controls (FDR < 0.05 and |fold change| > 1.8). (B) Fragments per kilobase of transcript per million (FPKM) values of indicated members of the Integrator complex in RNA-seq are shown. (C) Relative mRNA levels of indicated members of the Integrator complex in LK cells are shown. (D-F) GSEA plots show that transcriptional signatures associated with cell-cycle transition (D), apoptosis (E), and PRC2 targets (F) are dysregulated in *Ints11*<sup>Δ/Δ</sup> LK cells. The NES, *P*-value and FDR are shown. (G) FPKM values of genes associated with cell-cycle, apoptosis, and PRC2 targets in RNA-seq are shown. (H and I) Cell-cycle analysis of HSPCs from WT (*n* = 4) and *Ints11*<sup>Δ/Δ</sup> (*n* = 5) mice 72 hours after poly(I:C) injection. Representative flow cytometry plots (H), and percentages of cells in each stage (I) are shown. (J) Western blot showing the protein level of p21<sup>Cip1</sup> in LK cells 72 hours after first poly(I:C) injection. (K) Apoptosis analysis of HSPCs from WT (*n* = 4) and *Ints11*<sup>Δ/Δ</sup> (*n* = 5) mice 72 hours after poly(I:C) injection by Annexin V/7-AAD staining. Data are shown as the mean ± SEM. Unpaired Student's *t*-test; \**P* < 0.05, \*\**P* < 0.01, \*\*\**P* < 0.001.



**Fig. S5. Transcriptomic changes of HSPC populations in *Ints11*-deficient cKit<sup>+</sup> cells.** (A) UMAP visualization of LT-HSC, ST-HSC, MPP2, and MPP3 cells for WT and *Ints11*<sup>Δ/Δ</sup>, respectively. Each dot represents one cell, and cluster identity is color-coded (Seurat). (B) Percentages of each hematopoietic cluster in WT and *Ints11*<sup>Δ/Δ</sup> cKit<sup>+</sup> cells are shown. (C-E) Violin plots of erythrocyte/megakaryocyte (C), apoptosis (D), and proliferation (E) transcription signatures in indicated populations are shown. The scores were calculated based on the expression values for genes in given gene sets. (F) Cell cycle phase distributions in different populations of WT and *Ints11*<sup>Δ/Δ</sup> cells. (G and H) Violin plots showing the log-transformed normalized expression levels of *Gata2* (G) and *Cdkn1a* (H) in HSPC populations. Mann-Whitney U test; \**P* < 0.05, \*\**P* < 0.01, \*\*\**P* < 0.001, \*\*\*\**P* < 0.0001.

**A****B****C****D****E****F**

**Fig. S6. INTS11 interacts with the PRC2 complex.** (A) Genome-wide distribution of INTS11-enriched regions in hematopoietic cells (GSE106359). Regions that overlap in the two biological replicates are preserved. (B) Representative ChIP-Seq tracks show INTS11 and SUZ12 co-occupy the gene promoters in hematopoietic cells. (C) Schematic representation of the lentiviral vectors expressing mouse *Ints11* gene (FLAG-INTS11) and the empty vector (EV) control. RRE, Rev Response Element. SFFV, spleen focus-forming virus. WPRE, woodchuck hepatitis virus posttranscriptional regulatory element. (D) Reciprocal EZH2 IP from nuclear extracts of 293T cells transfected with FLAG-tagged INTS11 or EV, and representative immunoblot analysis is shown. Arrowhead indicates the FLAG-fusion protein. (E) Coomassie blue-stained gel shows the GST-INTS11 fusion protein and GST control. (F) The GST-INTS11 fusion protein was immobilized on glutathione-agarose beads and incubated with SUZ12 or EED, respectively. Immobilized GST protein was used as controls.

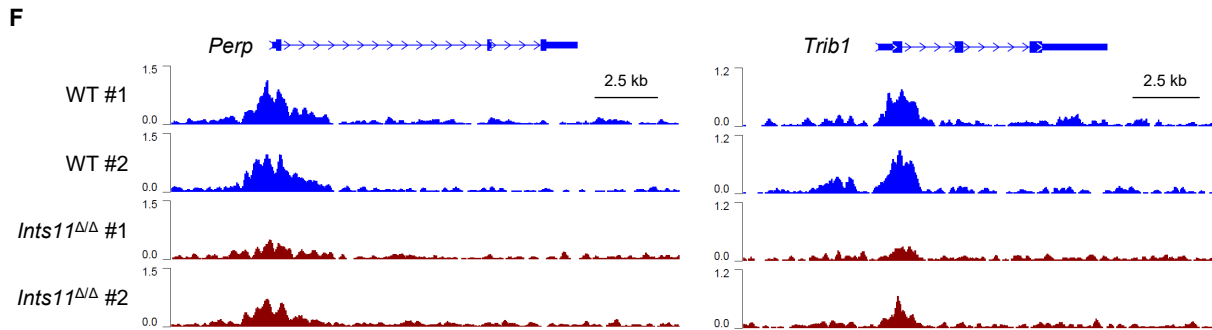
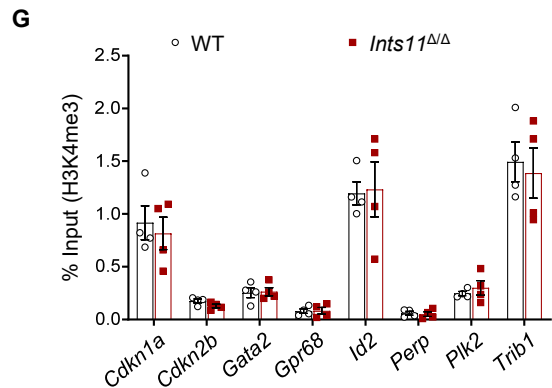
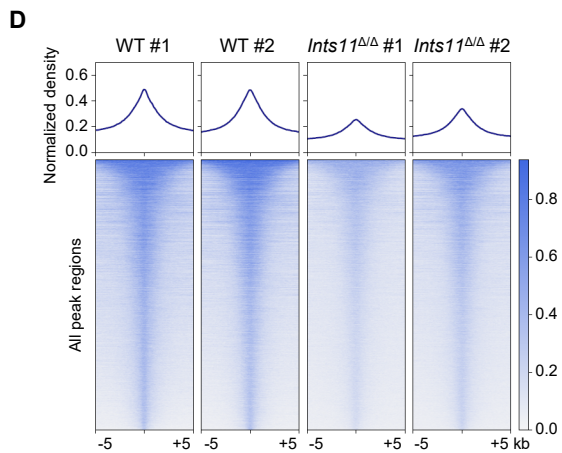
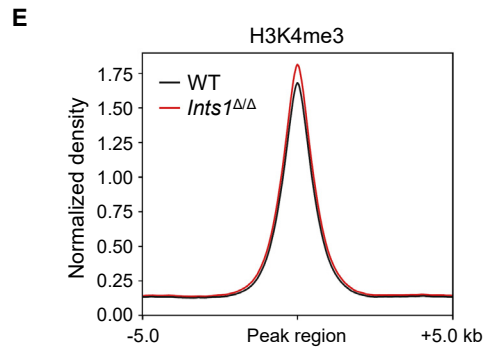
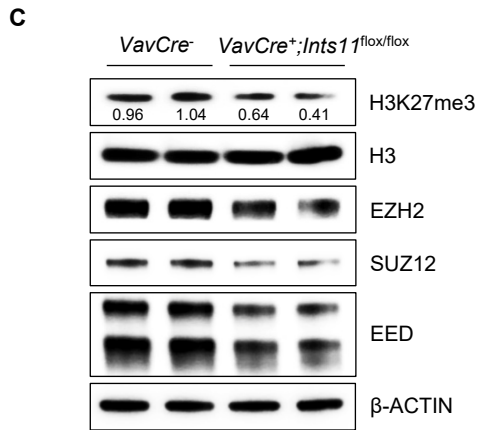
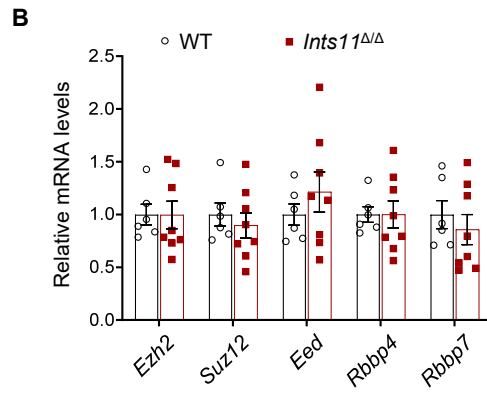
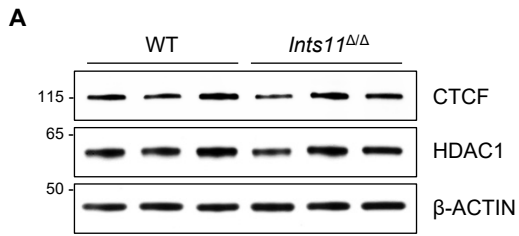


**Fig. S7. INTS11 deletion reduces the H3K27me3 enrichment by destabilizing the PRC2 complex.** (A) The protein levels of CTCF and HDAC1 in LK cells from WT and *Ints11*<sup>Δ/Δ</sup> mice 72 hours after first poly(I:C) injection are shown. (B) qPCR showing the mRNA expression levels of indicated members of PRC2 complex in LK cells. (C) Western blot analysis of H3K27me3 and indicated subunits of the PRC2 complex in fetal liver cells from *Vav1Cre*<sup>-</sup> and *Vav1Cre*<sup>+</sup>;*Ints11*<sup>flox/flox</sup> embryos at E13.5. H3 and β-ACTIN were used as loading controls. (D) Heatmaps of normalized H3K27me3 ChIP-seq read densities centered on the midpoints of all H3K27me3 regions. Each row represents a single region. (E) Global levels of H3K4me3 at peaks and 5-kb regions surrounding the peak midpoint. The coverages were normalized by the sequencing depth and averaged in 2 biological replicates. (F) Normalized H3K27me3 signals on *Perp* and *Trib1* gene loci are shown. (G) ChIP-qPCR showing the enrichment of H3K4me3 at the promoters of the genes in Fig. 4F ( $n = 4$  per genotype). Data are shown as the mean  $\pm$  SEM.

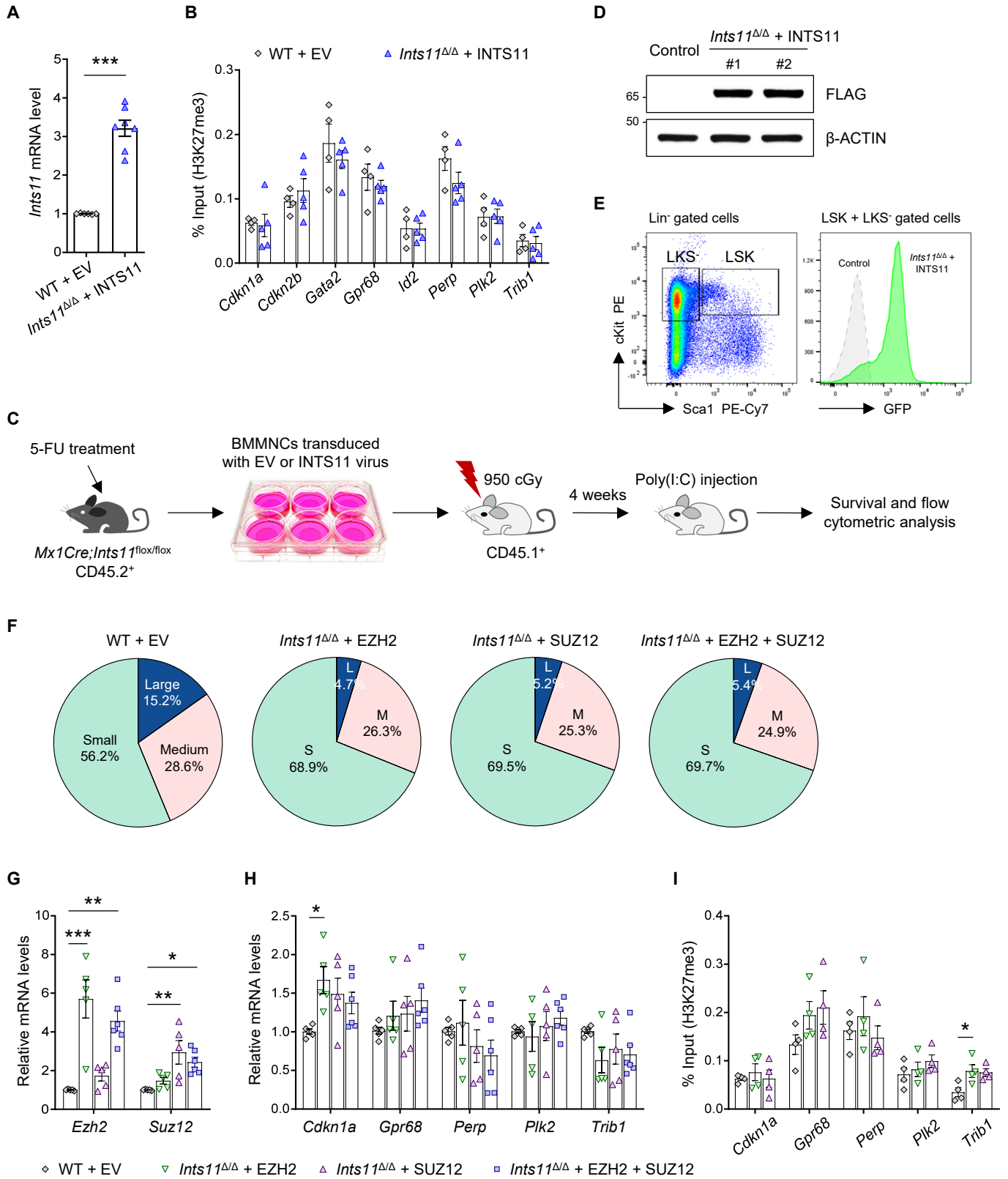




**Fig. S8. Re-expression of INTS11 increases the PRC2 activity and rescues the *Ints11*-deficient phenotypes.** (A) qPCR showing the mRNA levels of *Ints11* in *Ints11*<sup>Δ/Δ</sup> cells transduced with FLAG-INTS11. Each dot represents an individual mouse (*n* = 6 to 7 per group). (B) The enrichment of H3K27me3 at the promoters of the indicated genes in *Ints11*<sup>Δ/Δ</sup> cells transduced with FLAG-INTS11 (*n* = 4 to 5 per group). (C) Schematic representation of *in vivo* rescue assay. BM mononuclear cells from 5-FU treated *Mx1Cre*<sup>+</sup>;*Ints11*<sup>fllox/fllox</sup> mice (CD45.2<sup>+</sup>) were transduced with a lentiviral vector (FLAG-INTS11 or EV control) and then transplanted into lethally irradiated CD45.1<sup>+</sup> recipient mice. *Ints11* deletion was induced after 4 weeks of transplantation. (D) Western blotting showing the expression of FLAG-INTS11 in cKit<sup>+</sup> cells from recipient receiving *Ints11*<sup>Δ/Δ</sup> cells transduced with FLAG-INTS11. (E) Flow cytometric analysis of HSPC populations from recipients receiving *Ints11*<sup>Δ/Δ</sup> cells transduced with FLAG-INTS11 after 8 weeks of poly(I:C) injection. The population of HSPCs (LSK and LKS<sup>-</sup>) was restored and confirmed the expression of GFP in the recipient mice. (F) Pie-charts showing the proportion of colony size in *Ints11*-deficient cKit<sup>+</sup> cells transduced with PRC2 subunits (EZH2 and/or SUZ12). (G and H) qPCR showing the mRNA levels of *Ezh2* and *Suz12* (G) and PRC2 targets (H) in *Ints11*<sup>Δ/Δ</sup> cells transduced with EZH2 and/or SUZ12. Each dot represents an individual mouse (*n* = 5 to 6 per group). (I) The levels of H3K27me3 at the promoters of indicated PRC2 target genes are shown (*n* = 4 per group). Data are shown as the mean ± SEM. Unpaired Student's *t*-test, or one-way ANOVA with Tukey's multiple comparisons test; \**P* < 0.05, \*\**P* < 0.01, \*\*\**P* < 0.001.

**Table S1. Primers used in this study.**

Name	Forward	Reverse
Genotyping PCR		
<i>Ints11-flox</i>	ATGCCTACGTAAGGAAAGCAGACT	TGAGGTCTAGTGTTGAATGAAGCC
<i>Ints11-Rec</i>	GATGGCTCCTCAGCGTCATT	CTAGGCCACTGCCGGTTTAT
qPCR		
<i>Ints11</i>	TCATGTTGGACTGTGGGATG	TGGGTGATGTAAGAAAAGTCAGG
<i>Ints3</i>	GAGTTACAGAAGGGAAGGGGA	ACTGGTTGAAAGTAGCAGCCT
<i>Ints4</i>	CACCTGAAAAAGCGGGTGTAT	AATCGGAGCTTCTTGGTAGCA
<i>Ints7</i>	TCCGCTCTTATGGAAGTGGAC	AGGGAACGGGTACTTCTGGAA
<i>Ints9</i>	CCCCAGGCTATCTAATCTTCCC	AATCCACAAATACATGACCGGAG
<i>Ints10</i>	ACACCATCGAACGGAATGCC	GCTGGTCCGGGAAATTCACAA
<i>Ints13</i>	GTTGTGGATCACTGCCATAC	GGGAGCCAAAGGGATGATGC
<i>Ezh2</i>	ACTTCTGTGAGCTCATTGCG	CGACTGCATTCAGGGTCTTT
<i>Suz12</i>	CCAACGATAAGTCTACAGCTCC	GTAGTCAGCGTCTCCTAACAG
<i>Eed</i>	TCCACTTTCCTGACTTTTCTACC	CCATTTTGCCAGGTTTCCAG
<i>Rbbp4</i>	GACGACGCAGTGAAGAAC	CTGGGCAGTTAAGCTGGGC
<i>Rbbp7</i>	GAGCGTGCATCAACGAAGAG	CCACTGAACGGTAAGACTGGG
<i>Cdkn1a</i>	CCTGGTGATGTCGGACCTG	CCATGAGCGCATCGCAATC
<i>Cdkn2b</i>	CCCTGCCACCCTTACCAGA	CAGATACCTCGCAATGTCACG
<i>Gata2</i>	ATACCCACCTATCCCTCCTATG	AGCCTTGCTTCTCTGCTTAG
<i>Gpr68</i>	TATCTTGCCCCATCGACCACA	AGTACCCGAAGTAGAGGGACA
<i>Id2</i>	ATGAAAGCCTTCAGTCCGGTG	AGCAGACTCATCGGGTCGT
<i>Perp</i>	ATGGAGTACGCATGGGGAC	GGCGAAGAACGAGAGAATGAAG
<i>Plk2</i>	AGCCAGAAGTCCGATACTACC	TCCCTAGCTTGAGATCCCTGT
<i>Trib1</i>	AGAACCCAGCTTAGACTGGAA	AAAAGCGTATAGAGCATCACCC
ChIP-qPCR		
<i>Cdkn1a</i>	GCCCAAAGCGTGAGAATGAA	AAACAGGGCACTTGGTTCAC
<i>Cdkn2b</i>	GAAACATCCCTCGGCACTAG	GAGACATTGCTCCAGATAGC
<i>Gata2</i>	GTCCACAATCCCTAGACTCATG	AGCCCAAATCCAAGTACTC
<i>Gpr68</i>	TCTCTACCTTCTCCAGCT	TCCTGACCTAGAGACTGGCT
<i>Id2</i>	GCCTTTTATCCTCTTTCTCCCC	CACAAGCACATTACCGAAACG
<i>Perp</i>	ACCAAAGCTACCCGGATTAAG	CGGATCTACCTTTGGACCTTG
<i>Plk2</i>	CTTGGGCTCTCACTATCTGATC	TCCAGTTTTCTCGTTTCCCC
<i>Trib1</i>	TGGGTTTGGCAGAGCAGATA	CCACAGGAAAGCACTCAACC

**Table S2. Detailed list of reagents used in this study.**

Reagent or Resource	Source	Identifier
Antibodies		
Mouse lineage antibody cocktail APC	BD Pharmingen	Cat# 558074; RRID: AB 1645213
Rat monoclonal anti-mouse CD117 (cKit) PerCP-Cy5.5	BD Pharmingen	Cat# 560557; RRID: AB 1645258
Rat monoclonal anti-mouse CD117 (cKit) PE	BD Pharmingen	Cat# 553869; RRID: AB 395103
Rat monoclonal anti-mouse CD117 (cKit) APC	BD Pharmingen	Cat# 553356; RRID: AB 398536
Rat monoclonal anti-mouse Ly-6A/E (Sca1) PE-Cy7	BD Pharmingen	Cat# 558162; RRID: AB 647253
Rat monoclonal anti-mouse CD34 FITC	BD Pharmingen	Cat# 553733; RRID: AB 395017
Rat monoclonal anti-mouse CD34 Alexa Fluor 700	BD Pharmingen	Cat# 560518; RRID: AB 1727471
Rat monoclonal anti-mouse CD135 BV421	BD Pharmingen	Cat# 562898; RRID: AB 2737876
Rat monoclonal anti-mouse CD16/32 APC-Cy7	BioLegend	Cat# 101327; RRID: AB 1967102
Hamster monoclonal anti-mouse CD48 FITC	BD Pharmingen	Cat# 557484; RRID: AB 396724
Monoclonal anti-mouse CD150 PE	Thermo Fisher Scientific	Cat# 12-1502-82; RRID: AB 1548765
Rat monoclonal anti-mouse CD71 FITC	BD Pharmingen	Cat# 553266; RRID: AB 394743
Rat monoclonal anti-mouse CD71 PE	BD Pharmingen	Cat# 553267; RRID: AB 394744
Rat anti-mouse TER-119 APC	BD Pharmingen	Cat# 557909; RRID: AB 398635
Rat monoclonal anti-mouse Ly-6G and Ly-6C (Gr1) PerCP-Cy5.5	BD Pharmingen	Cat# 552093; RRID: AB 394334
Rat monoclonal anti-mouse Ly-6G and Ly-6C (Gr1) PE-Cy7	BD Pharmingen	Cat# 565033; RRID: AB 2739049
Rat monoclonal anti-mouse CD11b (Mac1) PE	BD Pharmingen	Cat# 553311; RRID: AB 394775
Rat monoclonal anti-mouse CD4 PerCP-Cy5.5	BD Pharmingen	Cat# 550954; RRID: AB 393977
Rat monoclonal anti-mouse CD4 PE-Cy7	BD Pharmingen	Cat# 552775; RRID: AB 394461
Rat monoclonal anti-mouse CD8a PE	BD Pharmingen	Cat# 553033; RRID: AB 394571
Rat monoclonal anti-mouse CD45R/B220 APC	BD Pharmingen	Cat# 553092; RRID: AB 398531
Mouse monoclonal anti-mouse CD45.2 PerCP-Cy5.5	BD Pharmingen	Cat# 552950; RRID: AB 394528
Mouse monoclonal anti-mouse CD45.1 FITC	BD Pharmingen	Cat# 553775; RRID: AB 395043
Mouse monoclonal anti-mouse CD45 PE-Cy7	BD Pharmingen	Cat# 552848; RRID: AB 394489

7-AAD	BD Pharmingen	Cat# 559925; RRID: AB 2869266
Rabbit polyclonal anti-INTS11	Bethyl Laboratories	Cat# A301-274A; RRID: AB 937779
Rabbit polyclonal anti-INTS1	Bethyl Laboratories	Cat# A300-361A; RRID: AB 2127258
Rabbit polyclonal anti-INTS3	Bethyl Laboratories	Cat# A302-050A; RRID: AB 1604272
Rabbit polyclonal anti-INTS4	Bethyl Laboratories	Cat# A301-296A; RRID: AB 937909
Mouse monoclonal anti- $\beta$ -Actin	MilliporeSigma	Cat# A2228; RRID: AB 476697
Rabbit monoclonal anti-mouse p21	Abcam	Cat# ab188224; RRID: AB 2734729
Rabbit polyclonal anti-H3K27me2	Cell Signaling Technology	Cat# 9728; RRID: AB 1281338
Rabbit polyclonal anti-H3K27me3	MilliporeSigma	Cat# 07-449; RRID: AB 310624
Rabbit polyclonal anti-H3K4me3	Diagenode	Cat# C15410003; RRID: AB 2616052
Rabbit polyclonal anti-H3	Abcam	Cat# ab1791; RRID: AB 302613
Rabbit monoclonal anti-EZH2	Cell Signaling Technology	Cat# 5246; RRID: AB 10694683
Mouse monoclonal anti-EZH2	MilliporeSigma	Cat# 17-662; RRID: AB 1977568
Rabbit monoclonal anti-SUZ12	Cell Signaling Technology	Cat# 3737; RRID: AB 2196850
Rabbit monoclonal anti-EED	Cell Signaling Technology	Cat# 85322
Rabbit polyclonal anti-RBBP4/7	Cell Signaling Technology	Cat# 4633; RRID: AB 1904116
Rabbit polyclonal anti-CTCF	MilliporeSigma	Cat# 07-729; RRID: AB 441965
Rabbit polyclonal anti-HDAC1	Thermo Fisher Scientific	Cat# PA1-860; RRID: AB 2118091
Mouse monoclonal anti-FLAG M2	MilliporeSigma	Cat# F3165; RRID: AB 259529
Mouse monoclonal anti-HA	MilliporeSigma	Cat# H3663; RRID: AB 262051
Mouse IgG, HRP-linked whole Ab (from sheep)	GE Healthcare	Cat# NA931; RRID: AB 772210
Rabbit IgG, HRP-linked F(ab') <sub>2</sub> fragment (from donkey)	GE Healthcare	Cat# NA9340; RRID: AB 772191
<b>Bacterial and Virus Strains</b>		
NEB 5-alpha Competent E. coli	NEB	Cat# C2987H
BL21 (DE3) Competent E. coli	NEB	Cat# C2527H
One Shot Stbl3 Chemically Competent E. coli	Thermo Fisher Scientific	Cat# C737303
<b>Chemicals, Peptides, and Recombinant Proteins</b>		
Poly(I:C)	InvivoGen	Cat# ttrl-pic-5
5-fluorouracil	Selleckchem	Cat# S1209
Methylcellulose medium MethoCult M3134	STEMCELL Technologies	Cat# 03134

Recombinant Murine Stem Cell Factor	Peprotech	Cat# 250-03
Recombinant Murine Interleukin 3	Peprotech	Cat# 213-13
Recombinant Murine Thrombopoietin	Peprotech	Cat# 315-14
Recombinant Murine Granulocyte-Macrophage Colony-Stimulating Factor	Peprotech	Cat# 315-03
Recombinant Human Erythropoietin	Peprotech	Cat# 100-64
Recombinant Human Interleukin-6	Peprotech	Cat# 200-06
Mouse CD45 MicroBeads	Miltenyi Biotec	Cat# 130-052-301
Mouse CD117 MicroBeads	Miltenyi Biotec	Cat# 130-091-224
Mouse Direct Lineage Cell Depletion Kit	Miltenyi Biotec	Cat# 130-110-470
Lipofectamine 3000 Transfection Reagent	Thermo Fisher Scientific	Cat# L3000075
TRIzol Reagent	Thermo Fisher Scientific	Cat# 15596026
Benzonase Nuclease	MilliporeSigma	Cat# E1014
Protease Inhibitor Cocktail Tablets	MilliporeSigma	Cat# S8830
Mouse monoclonal anti-FLAG M2 Affinity Gel	MilliporeSigma	Cat# A2220; RRID: AB 10063035
Mouse monoclonal anti-HA Magnetic Beads	Thermo Fisher Scientific	Cat# 88837; RRID: AB 2861399
Protein A/G PLUS-Agarose	Santa Cruz Biotechnology	Cat# sc-2003; RRID: AB 10201400
Dynabeads Protein G	Thermo Fisher Scientific	Cat# 10004D
Pierce Glutathione Agarose	Thermo Fisher Scientific	Cat# 16100
Recombinant EZH2 Protein Complex (human)	Active Motif	Cat# 31337
Recombinant human EZH2 protein	OriGene Technologies	Cat# TP302054
Recombinant human SUZ12 protein	OriGene Technologies	Cat# TP302362
Recombinant human EED protein	OriGene Technologies	Cat# TP319261
Promethues ProSignal Pico ECL Reagent	Genesee Scientific	Cat# 20-300
Promethues ProSignal Femto ECL Reagent	Genesee Scientific	Cat# 20-302
<b>Critical Commercial Assays</b>		
FITC BrdU Flow Kit	BD Pharmingen	Cat# 559619; RRID: AB 2617060
PE Annexin V Apoptosis Detection Kit I	BD Pharmingen	Cat# 559763; RRID: AB 2869265
QIAfilter Plasmid Maxi Kit	Qiagen	Cat# 12263
QuantiTect Reverse Transcription Kit	Qiagen	Cat# 205313
Fast SYBR Green Master Mix	Thermo Fisher Scientific	Cat# 4385617
Subcellular Protein Fractionation Kit	Thermo Fisher Scientific	Cat# 78840
TruSeq Stranded mRNA Library Prep	Illumina	Cat# 20020594
Chromium Single Cell 3' Reagent Kit (v3)	10x Genomics	Cat# PN-1000075
Chromium Single Cell B Chip Kit (v3)	10x Genomics	Cat# PN-1000154
MicroPlex Library Preparation Kit (v2)	Diagenode	Cat# C05010013
<b>Deposited Data</b>		
Bulk RNA-Seq data	This paper	GEO: GSE159403
Single-cell RNA-Seq data	This Paper	GEO: GSE159404
ChIP-Seq data	This Paper	GEO: GSE159402
INTS11 ChIP-Seq data	(16)	GEO: GSE106359
SUZ12 ChIP-Seq data	(29)	GEO: GSE59090
<b>Experimental Models: Cell Lines</b>		
Human: HEK 293TN cell	System Biosciences	Cat# LV900A-1

Human: K562 cell	ATCC	Cat# CCL-243
Experimental Models: Organisms/Strains		
Mouse: B6.Cg-Commd10Tg(Vav1-icre)A2Kio/J (Vav1-Cre)	The Jackson Laboratory	JAX: 008610; RRID: IMSR_JAX:008610
Mouse: B6.Cg-Tg(Mx1-cre)1Cgn/J (Mx1-Cre)	The Jackson Laboratory	JAX: 003556; RRID: IMSR_JAX:003556
Mouse: B6.SJL-Ptprca Pepcb/BoyJ (BoyJ)	The Jackson Laboratory	JAX: 002014; RRID: IMSR_JAX:002014
Mouse: Ints11 flox	This paper	
Recombinant DNA		
pSFFV-FLAG-E2A-GFP	This Paper	N/A
pSFFV-FLAG-INTS11-E2A-GFP (mouse)	This Paper	N/A
pLV-CMV-HA-EZH2-CMV-mCherry (mouse)	This Paper	N/A
pLV-CMV-HA-SUZ12-CMV-GFP (mouse)	This Paper	N/A
pET-GST-INTS11 (human)	This Paper	N/A
Other		
Suprose 6 Increase 10/300 GL	Cytiva	Cat# 29091596